Spin-Split Image-Potential-Induced Surface State on Ni(111)

F. Passek and M. Donath
Max-Planck-Institut für Plasmaphysik, EURATOM-Association, W-8046 Garching bei München, Germany
(Received 27 April 1992)

Spin-resolved inverse photoemission measurements of the $n=1$ image-potential-induced surface state on Ni(111) reveal a magnetic exchange splitting of 18 ± 3 meV. The size of the splitting is in accord with calculations within the one-step model of inverse photoemission assuming the barrier potential as spin independent, but taking into account the different energy positions of the spin-up and spin-down band-gap boundaries. It is shown that spin resolution in experiments enables detection of spin splittings considerably smaller than the linewidths of the spectral features.

PACS numbers: 73.20.−r, 75.30.Pd, 79.60.Cn

The magnetic exchange splitting of surface electronic states has attracted considerable interest in both theory and experiment because these states act as sensors of the surface magnetic properties that may be quite different from the corresponding bulk properties. Non-spin-resolved photoemission (PES) has detected occupied surface states on nickel as double-peak structures being interpreted as energetically separated minority- and majority-spin emissions [1]. Spin-resolved inverse photoemission (IPE) succeeded in detecting empty exchange-split surface states on Ni(110) [2] and Ni(001) [3]. The size of the observed splittings was found to be of the same order as the splittings of bulk states. The experiments were related to surface states whose wave functions are peaked within the topmost atomic layers. These states are caused by the broken symmetry at the surface and are derived from bulk bands. They usually appear in gaps of the projected bulk band structure and are therefore called crystal-induced surface states. A different kind of surface state has its origin in the long-range nature of the Coulomb potential. An electron approaching a conductive surface feels the attractive force of its own image charge. Provided the reflectivity of the surface is high the electron may be trapped between the bulk crystal barrier and the image-potential surface barrier giving rise to a Rydberg-like series of bound states: the image-potential-induced surface states [4]. The states are pinned to the vacuum level E_V with binding energies of less than 1 eV. The wave functions of the image states have their maximum well outside the topmost atomic layer therefore having only one small overlap with bulk states. As a consequence, typical linewidths of the states are 20 to 80 meV reflecting their long lifetimes [5]. In addition, image states are not expected to show spin splittings of the same size as bulk states or crystal-induced surface states. Calculations within the one-step model of inverse photoemission assume the image potential to be spin independent but take into account the spin-dependent energy positions of the band-gap boundaries that form the crystal barrier. As a result of these calculations, a spin splitting of 100 meV is expected for Fe(110) [6], 13 meV for Ni(001) [7], and 27 meV for Ni(111) [8]. A schematic potential diagram for Ni(111) is given in Fig. 1. It demonstrates the spin-dependent height of the crystal barrier due to the different energy levels of the band-gap boundaries. This results in slightly lower binding energy for the minority compared with the majority image state. Since a possible influence of a spin-dependent barrier potential [6,9] has not been taken into account in the calculation, the given numbers are lower limits for the expected spin splittings.

Experimentally, the $n=1$ image-potential-induced surface state has been discovered by IPE [10]. High-resolution two-photon-photoemission (2PPE) measurements were able to resolve the first three members of the Rydberg series [11]. As a result of the lack of spin resolution 2PPE failed to detect any spin splitting, because the intrinsic linewidths of the image states turned out to be larger than the spin splitting. Yet using fitting procedures an upper limit of 40 meV for a possible spin splitting was deduced for the $n=1$ image state on Ni(111) with its intrinsic linewidth of 84 meV [11]. IPE measurements are constrained by the state-of-the-art energy resolution of 300 to 400 meV. By using the electron spin polarization as an additional experimental parameter, how-

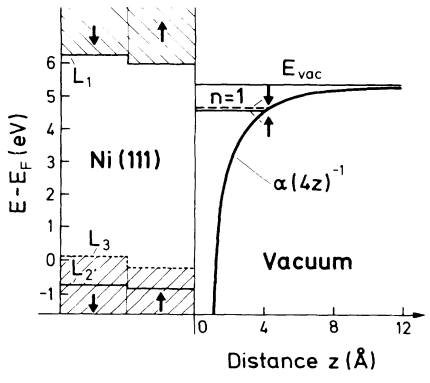

FIG. 1. Schematic potential diagram for image-potential surface states on Ni(111) indicating the image-potential barrier outside the crystal and the bulk *sp*-band gap between $L_{2'}$ and L_1 including the uppermost *d* band of symmetry L_3.

ever, the detection of spin splittings is not limited by the energy resolution or intrinsic linewidths, because both partial spin spectra are recorded *separately*. By this means, spin splittings of *sp*-derived bands, crystal-induced surface states [2,3], as well as adsorbate-induced states [2,12] have been detected. With regard to image-potential surface states two spin-resolved IPE studies have been carried out so far. On Ni(110), where the image-state emission is weak due to the lack of a bulk band gap, the adsorption of sulfur produced a well-pronounced spectral feature with a spin splitting of 32 ± 13 meV [13]. Unfortunately, no surface electronic structure calculation for the Ni/S system is available yet to evaluate this result. A study on clean Ni(001) revealed a hint for a nonzero splitting of the image state: $\Delta E = 13 \pm 13$ meV [3]. The present study was devoted to measure with high accuracy the magnetic exchange splitting of an image state on a clean ferromagnetic surface thereby testing the magnetic influence of the surface on the image state some angstroms in front of it. Ni(111) was chosen because of its well-pronounced image-state emission [14].

The apparatus for spin-resolved IPE and details about the measurement are published elsewhere [2,15]. Spin-polarized electrons are produced by photoemission from GaAs employing circularly polarized laser light. The photons emitted from the sample are detected in an iodine-SrF_2 bandpass counter ($\hbar\omega = 9.4 \pm 0.2$ eV) at an angle of 37° relative to the electron beam. The sample is a nickel single crystal cut into a hexagonal picture frame shape with its sides oriented along ⟨110⟩ directions and the [111] direction perpendicular to the hexagon plane. A remanently magnetized sample in a one-domain state, as proved by magneto-optical Kerr microscopy, was obtained by applying a high current pulse through a magnetization coil wound around one leg of the crystal. The Ni(111) surface was prepared by sputtering with 1.2-keV argon ions and subsequent annealing at 950 K. Low-energy electron diffraction and Auger electron spectroscopy were used to characterize the sample. All IPE spectra have been recorded at room temperature.

To get reliable IPE results on spin splittings a number of experimental details have to be under control. The work-function change of the GaAs photocathode resulting in an energy shift of the IPE spectrum was found to be smaller than 20 meV within 3 d. To avoid any artificial spin splitting as a result of this work function change the two partial spin spectra were measured quasisimultaneously by reversing the spin polarization about every 5 s for each value of the energy sweep with the magnetization kept fixed. To get good statistics several hundred single spectra were recorded and accumulated after having checked each single spectrum for any intensity change or energy shift. About every 45 min the sample had to be cleaned again. As a spin asymmetry of the apparatus, i.e., nonequivalence of spectra recorded with reversed spin polarization *and* sample magnetization, an energy shift of less than 5 meV was detected. To eliminate even this small effect half of the spectra were recorded with reversed magnetization.

IPE data for normal electron incidence on Ni(111) [inset of Fig. 2(a)] exhibit a prominent feature close to E_F due to transitions into bulk and surface states [14,16] and a structure at about 4.6 eV above E_F originating from the $n=1$ image state. Spin-resolved data of the image-state emission are displayed in Fig. 2(a) revealing a small but significant magnetic exchange splitting. The image state is underlayed by an almost linear background with a step-like increase at the high-energy side of the peak. This increase is due to the $n=2,3,\ldots$ members of the Rydberg

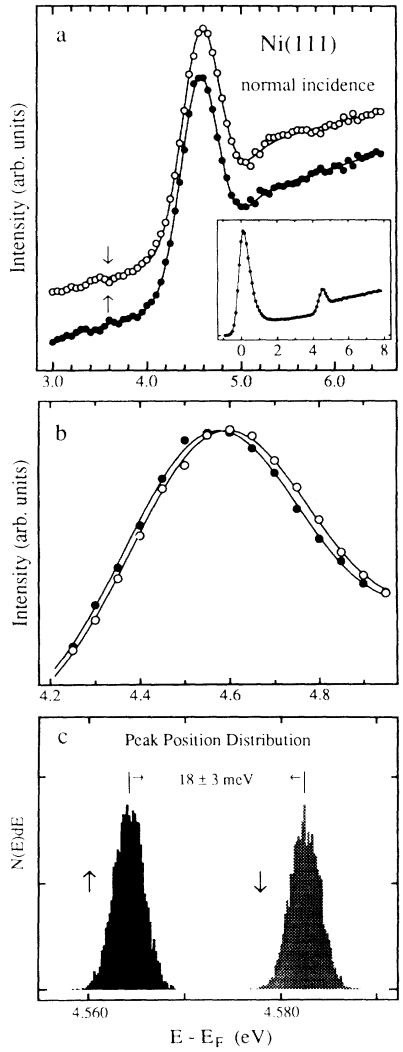

FIG. 2. (a) Spin-resolved inverse photoemission data ($\hbar\omega = 9.4$ eV, normal electron incidence) of the image-potential-induced surface state on Ni(111). Inset: Spin-integrated overview spectrum. (b) Same data on an enlarged energy scale with the spin-dependent background offset suppressed. The statistical uncertainty of the data points is within the size of the symbols. (c) Peak position distribution for spin-up and spin-down image-state emission (see text for details).

series with binding energies of less than 250 meV plus a steplike spectral feature at E_V already often observed in experiment [14,17] and reproduced by one-step model calculations [6]. In addition, the background intensity reflecting transitions of inelastically scattered electrons shows a spin-dependent, almost constant offset in the energy interval under consideration. This spin dependence is due to the high spin asymmetry of the density of empty states close to the Fermi level serving as final states. Figure 2(b) presents the data of Fig. 2(a) on an enlarged energy scale with suppressed spin-dependent background offset, showing unambiguously the spin splitting.

To extract the size of the splitting we determined the peak positions of spin-up and spin-down emission by a least-squares fitting procedure. The spectra are composed of a constant plus a linear background, the steplike background increase at E_V, and the Rydberg series of image states. Since the $n=1$ image state is known to have an intrinsic linewidth of 84 meV, the corresponding emission observed in IPE is dominated by the apparatus function (FWHM $\approx$ 400 meV) approximated by a Gaussian function. The higher members of the Rydberg series are not resolved and appear as a weak structure at about 5.15 eV at the low-energy side of the steplike increase (see also Fig. 3). Both the $n=2,3,\ldots$ image states and the steplike background increase are well reproduced by only one step function convoluted by the apparatus function. This structure was allowed to shift energetically to give the best fit. The fit curves are shown as solid lines through the data points in Figs. 2(a) and 2(b). The obtained peak positions are 4.5640 ± 0.0018 eV for spin-up and 4.5822 ± 0.0018 eV for spin-down spectrum resulting in a significant magnetic exchange splitting of 18.2 ± 2.5 meV. Note that this accuracy was only possible because all 70 data points per partial spin spectrum with up to 135000 counts per point contribute to the peak center determination.

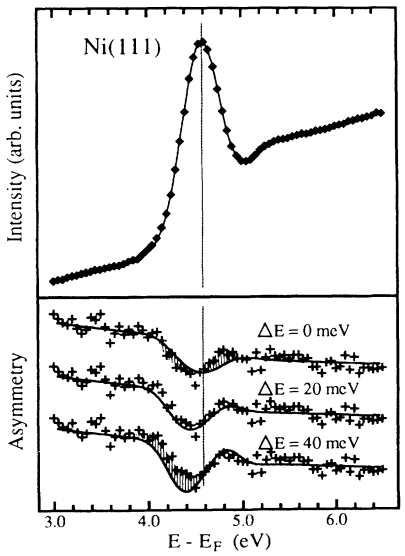

FIG. 3. Upper part: Spin-integrated inverse photoemission data of the image state on Ni(111) (diamonds) and a least-squares fit (solid line). Lower part: Spin asymmetry (crosses) varying from -13.7% to -7.5% within the shown energy range compared with simulated asymmetry curves (solid lines) obtained for three different splittings ΔE.

We are aware of the fact that a peak position determined by a fit depends critically on the chosen fit function. Therefore, besides the described fit function we tried also a Lorentzian function and a variable combination of a Gaussian and a Lorentzian function to fit the peak as well as different energy positions for the background increase to fit the background. In addition, we varied the energy interval for the fit. By doing so the absolute energy position of each partial spin emission varied within 30 meV. The relative difference between spin-up and spin-down peaks, however, was found to be between 18 and 20 meV within the error margins given above provided the same type of fit function was used for both partial spin spectra. This reasonable assumption is supported by the experimental finding that both partial spin emissions exhibit almost identical shapes [Fig. 2(a)].

To illustrate and confirm the error margins of only 2.5 meV for the spin splitting we produced a series of 3000 pseudoexperimental spectra by varying each measured data point randomly corresponding to the Gaussian distribution of its own statistical error. The peak positions for all these pseudoexperimental spectra have been determined by the fitting procedure described above. Figure 2(c) displays the peak position distributions for 3000 spin-up and spin-down spectra. The totally separated distributions illustrate in an impressive way the confidence level of the determined spin splitting which is by a factor of 5 smaller than the intrinsic linewidth and by a factor of 20 smaller than the experimental energy resolution.

In the following we use the spin asymmetry $A = (N_\uparrow - N_\downarrow)/(N_\uparrow + N_\downarrow)$ for an additional approach to confirm the observed spin splitting. Figure 3 shows spin-integrated IPE data of the image state (closed diamonds) and the spin asymmetry A (crosses) varying from -13.7% to -7.5% within the 3.5-eV energy range shown. In case a spectral feature is spin split one expects a plus-minus feature in the spin asymmetry. In our case, however, the image state is underlayed by a polarized background. By definition, an unpolarized peak on a polarized background produces a structure of A located at the maximum of the unpolarized peak [2]. A structure of A shifted in energy from the maximum of the peak, however, is a sensitive indicator of a spin splitting. To simulate spin splittings and their consequences for A we have duplicated the least-squares fit curve (solid line through spin-integrated data) and added (subtracted) an offset to get a "spin-up" ("spin-down") spectrum with realistic background intensity. Shifting these two spectra against one another in energy simulates an image state with variable exchange splitting. In the lower part of Fig. 3 the corresponding "asymmetry" curves (solid lines) for three

simulated splittings ($\Delta E = 0, 20, 40$ meV) are compared with the measured one (crosses). The asymmetry data are best described by a simulated splitting of 20 meV in agreement with the results obtained above. In particular, with increasing ΔE the energetical shift of the asymmetry dip and the development of a plus-minus feature is demonstrated. It should be noted that this method is only applicable in the case of almost identical line shapes for spin-up and spin-down curves. In general it cannot be used to deduce the exact value of the splitting.

In conclusion, the long-standing question about a possible spin splitting of the image-potential-induced surface state has been answered unambiguously by high-accuracy spin-resolved photoemission measurements. The magnetic exchange splitting of the $n=1$ image state on Ni(111) has been determined to 18 ± 3 meV. This value is about 10 times smaller than the spin splitting of the band-gap boundary L_1 and the splitting of a crystal-induced surface state on Ni(110) located in the same gap [2]. Nevertheless, the splitting can be understood as a consequence of the spin-split band-gap boundaries leading to a spin-dependent crystal barrier height relevant for the binding energies of electrons trapped in front of the surface. It is in accord with calculations assuming the barrier potential as spin independent. Consequently, the possible influence of a spin-dependent barrier potential on the splitting of image states seems to be negligible. In addition, in this work several ways are presented how to deduce a spin splitting that is considerably smaller than lifetime broadening and/or experimental energy resolution.

We are indebted to V. Dose, K. Ertl, W. von der Linden, and R. Schneider for stimulating discussions and to D. Scholl for reading the manuscript. We thank G. Güntherodt for lending the nickel crystal.

[1] E. W. Plummer and W. Eberhardt, Phys. Rev. B **20**, 1444 (1979); W. Eberhardt, E. W. Plummer, K. Horn, and J. Erskine, Phys. Rev. Lett. **45**, 273 (1980); J. L. Erskine, Phys. Rev. Lett. **45**, 1446 (1980).

[2] M. Donath, Appl. Phys. A **49**, 351 (1989); M. Donath, V. Dose, K. Ertl, and U. Kolac, Phys. Rev. B **41**, 5509 (1990).

[3] K. Starke, K. Ertl, and V. Dose, Phys. Rev. B **45**, 6154 (1992).

[4] P. M. Echenique and J. B. Pendry, J. Phys. C **11**, 2065 (1978); E. G. McRae, Rev. Mod. Phys. **51**, 541 (1979); P. M. Echenique and M. E. Uranga, Surf. Sci. **247**, 125 (1991).

[5] P. M. Echenique, F. Flores, and F. Sols, Phys. Rev. Lett. **55**, 2348 (1985); R. W. Schoenlein, J. G. Fujimoto, G. L. Eesley, and T. W. Capehart, Phys. Rev. Lett. **61**, 2596 (1988).

[6] G. Borstel and G. Thörner, Surf. Sci. Rep. **8**, 1 (1988).

[7] R. Schneider, K. Starke, K. Ertl, M. Donath, V. Dose, J. Braun, M. Grass, and G. Brostel, J. Phys. Condens. Matter **4**, 4293 (1992).

[8] R. Schneider (private communication).

[9] R. L. Kautz and B. B. Schwartz, Phys. Rev. B **14**, 2017 (1976).

[10] P. D. Johnson and N. V. Smith, Phys. Rev. B **27**, 2527 (1983); V. Dose, W. Altmann, A. Goldmann, U. Kolac, and J. Rogozik, Phys. Rev. Lett. **52**, 1919 (1984); D. Straub and F. J. Himpsel, Phys. Rev. Lett. **52**, 1922 (1984).

[11] N. Fischer, S. Schuppler, Th. Fauster, and W. Steinmann, Phys. Rev. B **42**, 9717 (1990).

[12] G. Schönhense, M. Donath, U. Kolac, and V. Dose, Surf. Sci. **206**, L888 (1988).

[13] M. Donath and K. Ertl, Surf. Sci. **262**, L49 (1992).

[14] A. Goldmann, M. Donath, W. Altmann, and V. Dose, Phys. Rev. B **32**, 837 (1985).

[15] U. Kolac, M. Donath, K. Ertl, H. Liebl, and V. Dose, Rev. Sci. Instrum. **59**, 1931 (1988).

[16] A spin-resolved IPE study on bulk and surface states of Ni(111) will be published elsewhere.

[17] F. J. Himpsel, Phys. Rev. B **43**, 13394 (1991).

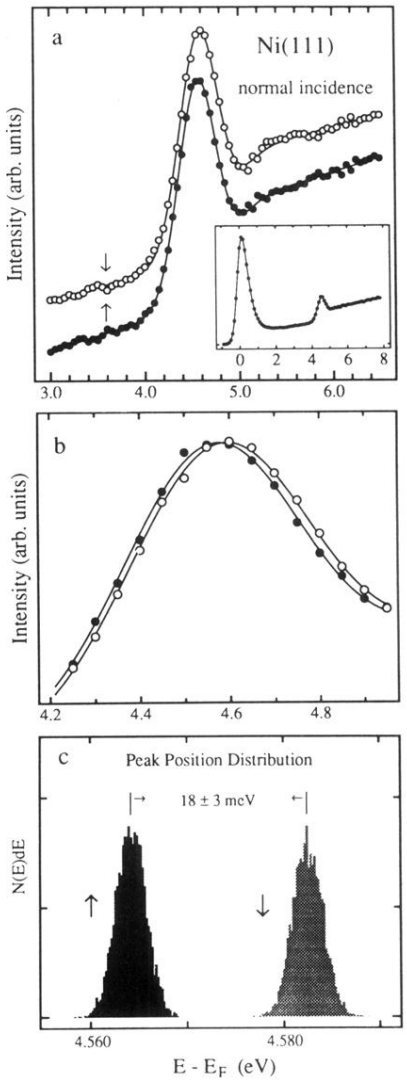

FIG. 2. (a) Spin-resolved inverse photoemission data ($\hbar\omega$=9.4 eV, normal electron incidence) of the image-potential-induced surface state on Ni(111). Inset: Spin-integrated overview spectrum. (b) Same data on an enlarged energy scale with the spin-dependent background offset suppressed. The statistical uncertainty of the data points is within the size of the symbols. (c) Peak position distribution for spin-up and spin-down image-state emission (see text for details).